ECMS for energy management of hybrid vessels via quasi-LPV control

Carlos Armenta, Rudy R Negenborn, Sébastien Delprat, G Hawksley

ECMS for energy management of hybrid vessels via quasi-LPV control

C. Armenta[a]*, S. Delprat[a], G. Hawksley[b], R.R. Negenborn[c]
[a]University Polytechnic Hauts-de-France, LAMIH UMR CNRS 8201, INSAHauts-de-France, INSA Hauts-de-France, F-59313 Valenciennes, France.
[b]Hybrid Marine Ltd
[c]Department of Maritime and Transport Technology, Delft University of Technology, Delft, the Netherlands
*Corresponding Author. Email: Carlosdaniel.Armentamoreno@uphf.fr

Synopsis

This work proposes a controller design that integrates an Equivalent Consumption Minimization Strategy framework and a quasi-LPV framework. The proposed scheme allows exploiting the characteristics of both frameworks. Also, a proof of the input-state-stability (ISS) of the closed-loop is presented, expressed as linear-matrix-inequality conditions. Simulation results are provided to illustrate the applicability of our approach in a hybrid powertrain setting as encountered in the maritime industry.

Keywords: Energy management, Marine vehicles, Optimal Control.

1. Introduction

REDUCING energy consumption and emissions of the marine industry nowadays has become a priority. Powertrain hybridization is one of the approaches to achieve these goals (Miyazaki et al., 2016). A hybrid powertrain uses at least two energy sources, with at least one reversible one, su ch as a battery. During vessels operations, the propulsion power request needs to be split between the different energy converters (genset, engine, electric machine, fuel cell, etc.) and storage (battery, super-capacitor). An energy management algorithm (EMA) is adopted to compute this power split and to minimize a criterion such as CO2 emissions while managing the energy storage level (e.g., the battery state of charge (SOC)) and to consider several constraints induced by the powertrain architecture and component sizing (Sciberras et al., 2016). If operational and environmental details of a mission are known a priori, the energy management problem can be formulated as an optimal control problem. Dynamic Programming (DP) (Bai et al., 2020; Wang et al., 2019) and Pontryagin's Minimum Principle (PMP) are widespread approaches to derive an optimal solution to hybrid powertrain energy management problems, even though alternative approaches based on the calculus of variations have been considered (East and Cannon, 2019). Dynamic Programming requires discretizing both the state and the time. Extensive search in the resulting grid allows approximating the optimal solution. This approach allows easily integrating state constraints, but it is only suitable for a limited number of states due to the so-called curse of dimensionality. Pontryagin's Minimum Principle (PMP) allows formulating optimality conditions in continuous-time, which boils down to consideration of a Boundary Value Problem (BVP) that can be solved using an appropriate solver. The resulting algorithm is, in general, faster than Dynamic Programming. In this work, PMP is considered since it allows deriving a real-time suboptimal, but efficient control algorithm referred to as the Equivalent Consumption Minimization Strategy (ECMS) (Sampathnarayanan et al., 2014; Xie et al., 2021).

Both the offline PMP and the real-time ECMS compute the control as a solution to the instantaneous minimization of the Hamiltonian associated with the optimal control problem. This Hamiltonian is defined as the sum of the fuel consumption and the state dynamics multiplied by a co-state. Within the ECMS framework, this Hamiltonian is denoted as total equivalent consumption. PMP optimality conditions provide the optimal dynamics of the co-state, and the initial value of the co-state can only be computed in simulation over known missions. In real-time, adaptive-ECMS replaces this optimal dynamic by a real-time closed-loop control approach of the energy storage level (typically the SOC) (Onori et al., 2011). Two main problems arise: how to design the controller and

Author's Biography
Carlos Armenta was born in Guasave Sinaloa, Mexico in 1994. He received M.S. from the Sonora Institute of Technology, Mexico. He is currently pursuing his Ph.D. degree in Automatic Control from the Polytechnic University Hauts-de-France, Valenciennes, France. His research interests are Energy Management Algorithms, Optimal control, Linear Matrix Inequalities and SOS techniques.
Sébastien Delprat received his PhD in 2002 and became assistant professor at the University of Valenciennes and Hainaut Cambresis. His research activities are dedicated to vehicle control, and especially hybrid vehicle energy management.
Graeme Hawksley was born in Liverpool, UK in 1959. He was awarded an MSc in microelectronics (hybrid control methods) from Bolton University in 2005. He formed Hybrid Marine Ltd in 1999 to conduct research and development into marine hybrid systems, and was granted three patents for hybrid control methods. He presents widely at international boat shows and part of the EU ISHY project (Implementation of Ship Hybridisation).
Prof. Dr. Rudy R. Negenborn is full professor in Multi-Machine Operations & Logistics at Delft University of Technology. He is head of the Section Transport Engineering & Logistics and of the Researchlab Autonomous Shipping. Negenborn's research interests include automatic control and coordination of transport technology (including autonomous vessels). He has over 200 peer reviewed academic publications, and leads NWO, EU and industry funded research.

how to prove the closed-loop stability. Various controllers have been investigated, such as PI, fuzzy, or predictive controllers, but only a few of them are provided with a closed-loop stability proof (Sampathnarayanan et al., 2014).

The contribution of this paper is to present a new controller that benefits from the ECMS framework and the underlying PMP optimal control theory. It is designed using the quasi-Linear Parameters Varying (LPV) approach, and it comprises a nonlinear state feedback control law coupled with a state observer. The Input-to-State Stability (ISS) of the closed loop is demonstrated (Sontag and Wang, 1996). This paper is organized as follows. In Section II, the considered hybrid vessel is introduced, and the formulation of its optimal control using PMP is given. In Section III, the real-time powertrain control is introduced. The system dynamics are modeled using the quasi-LPV control framework (Wang and Tanaka, 2004) and a Parallel Distributed Control law along with a state observer is designed. Simulation results are provided in Section IV. Section V concludes this paper and provides directions for future research.

2. Hybrid vessel optimal control

Powertrain energy management can be studied using quasi-static models for energy converters. The only dynamics considered are then those of the energy storage (Guzzella and Sciarretta, 2005). In this paper, we consider the simplified series hybrid vessel depicted in Fig. 1; which is made up of a traction motor, connected to the propeller; a battery pack, with a DC/DC converter; and a fuel cell, with auxiliaries. In order to formalize the dynamics, let w denote the power to be provided for the propulsion, y the power provided to/from the battery, u the fuel cell output power, and p the power consumed by the fuel cell auxiliaries.

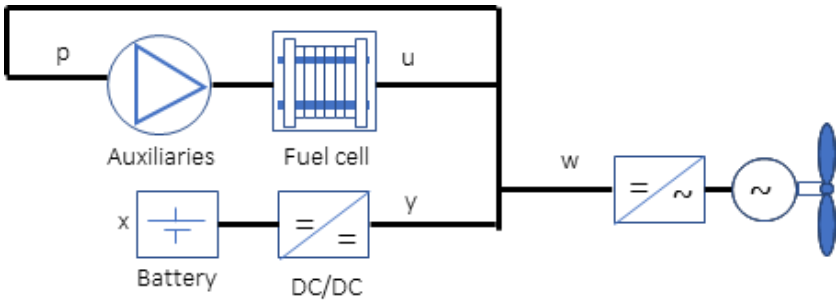

Fig. 1: Powertrain architecture

The mission profile $w(t)$ is the DC power to be provided to the traction motor as a function of time t. It may be computed from a speed profile and a vessel model as described in (Haseltalab et al., 2016). Alternatively, in this paper, we use data recorded on an existing sightseeing barge. The considered 6-days long mission profile is given in Fig. 2. For the considered optimal control problem, the mission is assumed to be of fixed length T and known of the optimization horizon $[0,T]$. This study investigates a possible fuel cell retrofit of the barge such that it could be operated on hydrogen and electricity from the batteries.

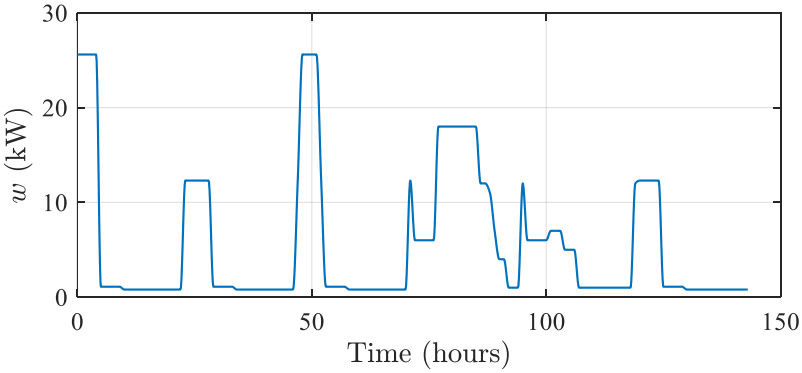

Fig. 2: Considered mission profile

Notation: When there is no ambiguity, the time dependence is omitted. The partial derivative with respect to a variable is denoted using a subscript. For instance, H_x denotes the partial derivative of H with respect to x.

The power split is given by:

$$w = y + u - p \tag{1}$$

Both the battery power y and the fuel cell output power u are limited:

$$y(t) \in [y_{\min}, y_{\max}] \tag{2}$$

$$u(t) \in [u_{\min}, u_{\max}] \tag{3}$$

Over an optimization horizon $[0, T]$, the hydrogen consumption to be minimized is assumed to be a quadratic function of the fuel cell produced power u (Tazelaar et al., 2012):

$$m_f = \int_0^T l(u)\,dt \tag{4}$$

$$l(u) = a + bu + cu^2 \tag{5}$$

The fuel cell auxiliaries electric consumption is estimated using the following loss model (Tazelaar et al., 2012):

$$p = \gamma_0 + \gamma_1 u \tag{6}$$

Combining (1)-(3) and (6), the feasible set $\left[\underline{u}(w), \bar{u}(w)\right]$ of the fuel cell output power can be determined:

$$\bar{u}(w) = \min\left(u_{\max}, \max\left(u_{\min}, \frac{w + \gamma_0 - y_{\min}}{(1-\gamma_1)}\right)\right) \tag{7}$$

$$\underline{u}(w) = \max\left(u_{\min}, \max\left(u_{max}, \frac{w + \gamma_0 - y_{\max}}{(1-\gamma_1)}\right)\right) \tag{8}$$

The battery coupled to the DC/DC converter is modeled using a simple voltage generator with a resistance in series (Gao et al., 2021; Oncken and Chen, 2020):

$$I_{batt} = \frac{E - \sqrt{E^2 - 4Ry}}{2R} \tag{9}$$

The open circuit voltage E and the internal resistance R are assumed to be constant. The battery SOC dynamics is :

$$\dot{x}(t) = f(u, w) \tag{10}$$

With $f(u, w) = \dfrac{-I_{batt}(t)}{Q} = \dfrac{-E + \sqrt{E^2 - 4Ry}}{2QR}$.

Two additional constraints on the SOC are considered:

$$x(0) = x_0 \tag{11}$$

$$x(T) = x_T \tag{12}$$

with x_0 and x_T as the initial and final SOC, respectively.

Equations (1)-(12) represent the optimal control problem to be solved. Several approaches can be considered to solve it. With $\lambda(t)$ the co-state, the Hamiltonian associated with the optimal control problem is formulated as:

$$H(u, \lambda, w) = l + \lambda f(u, w). \tag{13}$$

The optimal control policy can now be denoted by Π :

$$u = \Pi(\lambda, w) \tag{14}$$

$$\Pi(\lambda, w) = \underset{\nu \in \left[\underline{u}(w), \bar{u}(w)\right]}{\arg\min}\ H(\nu, \lambda, w) \tag{15}$$

The optimal co-state dynamics is then:

$$\dot{\lambda} = -H_x = 0. \tag{16}$$

Let us denote $Y = [x, \lambda]^T$, the BVP to be solved is:

$$\dot{Y} = \left[g(\lambda, w), 0\right]^T \tag{17}$$

$$d\left(x(0), x(T)\right) = 0, \tag{18}$$

where $d\left(x(0),x(T)\right)=\left(x(0)-x_0,x(T)-x_T\right)$ and the optimal state dynamics is:

$$g(\lambda,w)=f\left(\Pi(\lambda,w),w\right). \tag{19}$$

The BVP (17)-(18) can be solved using a dedicated solver (Kitzhofer et al., 2010) or using a simple bi-section search (Armenta et al., 2022).

Table 1 : Parameters values

Parameter	Value
$(y_{\min},y_{\max})$	$(-30\ kW, 30\ kW)$
$(u_{\min},u_{\max})$	$(0\ kW, 15\ kW)$
(E,R,Q)	$(105.3\,V, 0.985\ m\Omega, 2813 Ah)$
(a,b,c)	$\left(7.48\cdot10^{-6}, 6.97\cdot10^{-6}, 7.40\cdot10^{-7}\right)$
(γ_0,γ_1)	$\left(6.3\cdot10^{-5}, 0.125\right)$

As an illustration, let us consider a powertrain whose parameters are shown in Table 1. The BVP has been solved for $x(0)=1$, $x_T=0.2$. The initial co-state is $\lambda(0)=$ -18.94 . Fig. 3 depicts the optimal control result. The obtained hydrogen consumption is 27.8 kg and the final SOC is $19.99\,\%$. It should be noticed that the studied optimal control problem does not include any SOC limits. As a result, the SOC is allowed to reach negative values, and its corresponding fuel consumption will be interpreted as a lower bound as it does not have physical meaning (Interested readers may refer to state constrained PMP studied in (Hermant, 2008) or to PMP with state penalties (Sanchez and Delprat, 2018)). This result emphasizes that real-time powertrain operations should not be performed using a constant co-state, but a SOC feedback controller.

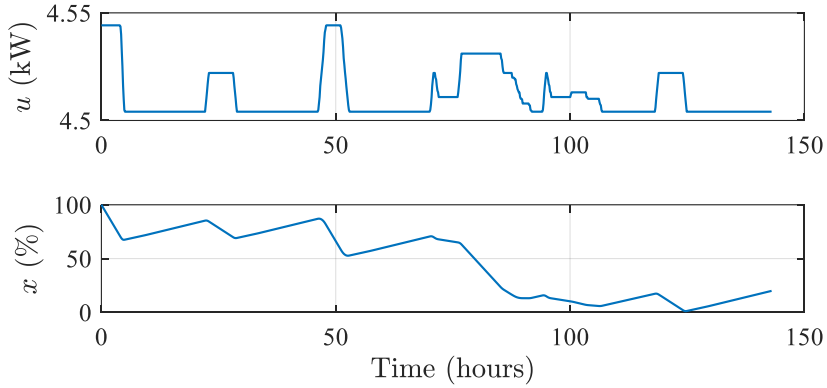

Fig. 3: Optimal control results for $x(0)=1$ and $x(T)=0.2$

3. Real-time control

During real-time operation, the future values of the mission profile and the mission length are unknown. The considered energy management consists of minimizing the hydrogen consumption while regulating the SOC nearby a reference setpoint. This reference setpoint can be either a constant or may follow a discharge profile when the battery is large enough to ensure the vessel operation in pure electric mode for a period of time long enough (plugin operations). If additional information on the mission is available, then more elaborated strategies can be adopted. It should be noticed that the considered problem involves not only the state-of-charge (SOC) tracking but also the energy management (i.e. ensuring energy-efficient powertrain operations). In this work, these two aspects are tackled (i) using the quasi-LPV literature for the controller synthesis and for demonstrating the closed-loop stability and performances (ii) using the Hamiltonian minimization (based on optimal policy (14)) within the control scheme to ensure an efficient energy management.

3.1. *Control structure*

Due to the control saturation (2)-(3) , not all the co-state values are of interest for SOC control. Let us restrict the co-state to $\lambda_{\min}(w) < \lambda < \lambda_{\max}(w)$, such that $g_\lambda(\lambda, w) < \varepsilon$, with ε small negative constant. As an example, $\lambda_{\min}(w)$ and $\lambda_{\max}(w)$ have been computed for the parameters given in Table 1. They are depicted with a green and red line in Fig. 4.

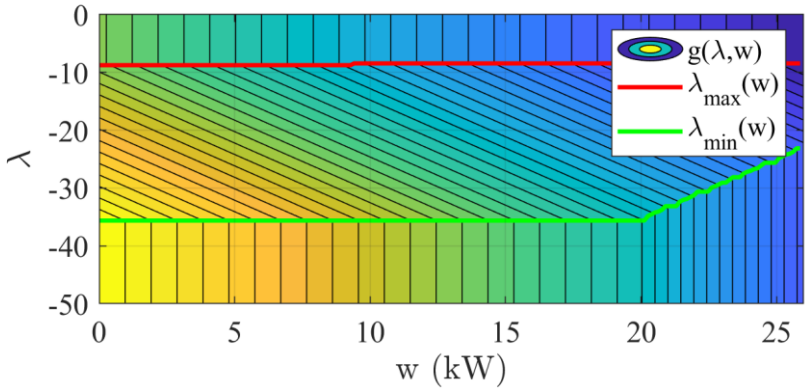

Fig. 4: State dynamics $g(\lambda, w)$

The following assumptions are considered. The mission profile w is differentiable with $\|\dot{w}\| < d_w$. The SOC reference x_{ref} is a piecewise linear function of time, so $\ddot{x}_{ref} = 0$ holds almost everywhere. Additionally, the assumptions from Lemma 1 of (van Keulen et al., 2014) are also considered but restricted to $\lambda_{\min}(w) < \lambda < \lambda_{\max}(w)$: l is a convex function in u and f is a strictly concave and strictly monotonically decreasing function in u.

Let $e = x - x_{ref}$ be the tracking error. The dynamic to be controlled is:

$$\dot{e}(t) = g\left(\lambda(t), w(t)\right) - \dot{x}_{ref} \tag{20}$$

To design a controller for (20), first, we consider the time derivative of (20) as follows:

$$\ddot{e} = g_\lambda(\lambda, w)\cdot\dot{\lambda} + g_x(\lambda, w)\cdot\dot{x} + g_w(\lambda, w)\cdot\dot{w} - \ddot{x}_{ref} \tag{21}$$

Since $g_x = 0$ and $\ddot{x}_{ref} = 0$, (21) can be simplified:

$$\ddot{e} = g_\lambda(\lambda, w)\cdot\dot{\lambda} + g_w(\lambda, w)\cdot\dot{w} \tag{22}$$

Let us introduce v as a new control with:

$$\lambda = sat\left(\int_0^t v(\tau)\,d\tau, \lambda_{\min}(w), \lambda_{\max}(w)\right), \tag{23}$$

where $sat(a,b,c) = \min\left(b, \max(a,c)\right)$. In practice, (23) should be implemented using an anti-windup scheme. The following state space representation is considered:

$$\begin{pmatrix}\ddot{e}\\ \dot{e}\end{pmatrix} = \begin{pmatrix}0 & 0\\ 1 & 0\end{pmatrix}\begin{pmatrix}\dot{e}\\ e\end{pmatrix} + \begin{pmatrix}g_\lambda(\lambda, w)\\ 0\end{pmatrix}\cdot v + \begin{pmatrix}g_w(\lambda, w)\\ 0\end{pmatrix}\cdot\dot{w}. \tag{24}$$

The derivative of the mission profile $\dot{w}$ is in general not available. It will be treated as a norm bounded disturbance.

3.2. *Controller design*

Let us introduce a more compact notation for the system (24) :

$$\begin{cases}\dot{X} = AX + B(\lambda, w)\cdot v + D(\lambda, w)\cdot d\\ x = CX\end{cases} \tag{25}$$

with $X = \begin{pmatrix}e\\ \dot{e}\end{pmatrix}$, $A = \begin{pmatrix}0 & 0\\ 1 & 0\end{pmatrix}$, $B = \begin{pmatrix}g_\lambda(\lambda, w)\\ 0\end{pmatrix}$, $D = \begin{pmatrix}g_w(\lambda, w)\\ 0\end{pmatrix}$, $C = \begin{pmatrix}0 & 1\end{pmatrix}$, $d = \dot{w}$.

The quasi-LPV provides a methodology to stabilize a wide range of nonlinear systems in a systematic way. According to Lemma 1 of (van Keulen et al., 2014), $z = g_\lambda(\lambda, w)$ is upper bounded. In order to formulate the system dynamic as a quasi-LPV model, let us consider a non-linear sector $z \in [z_1, z_2]$ with $z_1 < z_2 \le \varepsilon < 0$ and x as the measured and controlled output (Tanaka and Wang, 2001):

$$\begin{cases} \dot{X} = AX + \sum_{i=1}^{2} h_i(z) B_i v(t) + Dd = AX + B_h v(t) + Dd \\ x = CX \end{cases} \tag{26}$$

with $B_i = \begin{pmatrix} z_i \\ 0 \end{pmatrix}$, $h_1(z) = \dfrac{z_2 - z}{z_2 - z_1}$, $h_2(z) = 1 - h_1(z)$.

There exists an extensive literature on quasi-LPV control to deal with systems with the form of (26). A very simple control law is used but of course, many other alternatives are available (robust control, non-quadratic stability (Abdelkrim et al., 2019), etc.).

In order to stabilize the system (26) let us consider a PDC control law (Tanaka and Wang, 2001). It has the following form:

$$v = \sum_{i=1}^{2} h_i(z) F_i \hat{X}\,, \tag{27}$$

with F_i as the gains to be determined and $\hat{X}$ an estimate of the state X computed using a linear observer of the form:

$$\begin{cases} \dot{\hat{X}} = A\hat{X} + B(\lambda, w)v + L(x - \hat{x}) \\ \hat{x} = C\hat{X} \end{cases} \tag{28}$$

with L as the observer gain. Let $e_o = X - \hat{X}$ be the observer error whose dynamics is

$$\dot{e}_o = (A - LC)e_o + D(\lambda, w)d\,. \tag{29}$$

Considering (26) and (29) , we obtain

$$\dot{\tilde{X}} = \sum_{i=1}^{2}\sum_{j=1}^{2} h_i(z) h_j(z) G_{ij} \tilde{X} + \bar{D}d = G_h \tilde{X} + \bar{D}d \tag{30}$$

Where $\tilde{X} = \begin{bmatrix} X \\ e_o \end{bmatrix}$, $G_{ij} = \begin{bmatrix} A + B_i F_j & -B_i F_j \\ 0 & A - LC \end{bmatrix}$, and $\bar{D} = \begin{bmatrix} D \\ D \end{bmatrix}$.

In the particular case $d(t) = 0$, computing the gain F_j and L for the closed loop (30) stabilization using Linear Matrix Inequalities (LMI) is straightforward using classical matrix manipulations (Boyd et al., 1994; Tanaka and Wang, 2001). Then, our goal is to prove the ISS stability of the system (30) in the presence of a disturbance d .

Proposition. Let us consider the system dynamics (26) with the nonlinear control law (27) and observer (28), then, the origin $\tilde{X} = 0$ of the closed-loop dynamics (30) is ISS with a decay rate α and input constraint $|v| \le \mu$, for a scalar $\mu > 0$ and initial condition X_0, if there exist matrices $P_1 > 0$, $P_2 > 0$, L, M_i, $i \in \{1, 2, ..., r\}$, of suitable size, such that

$$\begin{aligned} &S_{11} < 0, \\ &S_{11} - S_{12} S_{22}^{-1} S_{12}^T < 0, \\ &\begin{bmatrix} 1 & X_0^T \\ X_0 & P_1^{-1} \end{bmatrix} > 0, \quad \begin{bmatrix} P_1^{-1} & M_i^T \\ M_i & I\mu^2 \end{bmatrix} > 0, \end{aligned} \tag{31}$$

where $S_{11} = AP_1^{-1} + B_i M_j + (*) + \alpha P_1^{-1}$, $S_{12} = -B_i M_j P_1^{-1}$, $S_{22} = \beta\left[P_2^{-1}(A - LC) + (*) + \alpha P_2^{-1}\right]$, with controller gains $F_i = M_i P_1$ and observer gain L .

Proof. Considering $d(t) = 0$, let us prove that the origin $\tilde{X} = 0$ of the system is asymptotically stable with a decay rate α . Taking a quadratic Lyapunov function as:

$$V(\tilde{X}) = \tilde{X}^T P \tilde{X} = \tilde{X}^T \begin{bmatrix} P_1 & 0 \\ 0 & \beta P_2 \end{bmatrix} \tilde{X}\,.$$

Let $\sigma_{\min P}$ and $\sigma_{\max P}$ be the smallest and largest eigenvalue of P. The proof of the stability condition (31) is trivial and is given in (Yoneyama et al., 2000). Since the system is asymptotically stable with a decay rate α, we have:

$$\tilde{X}^T\left(G_h{}^T P + PG_h\right)\tilde{X} \le -\alpha \tilde{X}^T P \le -\alpha\sigma_{\min P}\left|\tilde{X}\right|^2. \tag{32}$$

Now, let us consider $d(t) \neq 0$. If there exist $\mathcal{K}$ -functions ϕ_i, $i \in \{1,2,3,4\}$ such that $\phi_1\left(\left|\tilde{X}\right|\right) \le V\left(\left|\tilde{X}\right|\right) \le \phi_2\left(\left|\tilde{X}\right|\right) \forall \left|\tilde{X}\right| \in \mathbb{R}^n$

and $\dot{V}\left(\left|\tilde{X}\right|,|d|\right) \le -\phi_3\left(\left|\tilde{X}\right|\right) + \phi_4\left(|d|\right)$ then the system is ISS (Sontag and Wang, 1996). The first condition is fulfilled, since $\sigma_{\min P}\|x\|^2 \le x^T P x \le \sigma_{\max P}\|x\|^2$ for any quadratic Lyapunov function. To prove the second condition, let us consider the derivative of the Lyapunov function:

$$\begin{aligned}\dot{V}(x) &= \tilde{X}^T\left(G_h{}^T P + PG_h\right)\tilde{X} + d^T\bar{D}^T P\tilde{X} + \tilde{X}^T P\bar{D}^T d < -\alpha\sigma_{\min P}\left|\tilde{X}\right|^2 + d^T\bar{D}^T P\tilde{X} + \tilde{X}^T P\bar{D}d \\ &< -\alpha\sigma_{\min P}\left|\tilde{X}\right|^2 + 2\left|P\bar{D}\right|\left|\tilde{X}\right||d| = -\alpha\sigma_{\min P}\left|\tilde{X}\right|^2 + 2\delta\left|\tilde{X}\right||d| = -\alpha\sigma_{\min P}\theta\left|\tilde{X}\right|^2 + 2\delta\left|\tilde{X}\right||d| - \alpha\sigma_{\min P}(1-\theta)\left|\tilde{X}\right|^2,\end{aligned} \tag{33}$$

where $0 < \theta < 1$, and $\delta = \left|P\bar{D}\right| = \sigma_{\max P}\sqrt{2\partial g / \partial w_{\max}}$. Now considering the following inequality:

$$-\alpha\sigma_{\min P}\theta\left(\left|\tilde{X}\right| - \frac{\delta}{\alpha\lambda_{\min P}\theta}|d|\right)^2 < 0 \Leftrightarrow 2\delta|d|\left|\tilde{X}\right| < \alpha\sigma_{\min P}\theta\left|\tilde{X}\right|^2 + \frac{\delta^2}{\alpha\sigma_{\min P}\theta}|d|^2 \tag{34}$$

Finally, substituting (34) into (33) and taking $\phi_3\left(\left|\tilde{X}\right|\right) = -\alpha\sigma_{\min P}(1-\theta)\left|\tilde{X}\right|^2$ and $\phi_4\left(|d|\right) = |d|^2\,\delta^2 / \alpha\sigma_{\min P}\theta$, the second condition is fulfilled.

Remark. From the first inequality in (31), matrices M_i, $i \in \{1,2\}$, can be obtained. In the second inequality, by fixing negative poles for the linear observer, β can be chosen large enough such that (31) holds. The proposition above implies that the LMI conditions allow designing the observer and the controller separately and moreover the origin $\tilde{X} = 0$ of the closed-loop system (30) is ISS.

Finally, the control design procedure is : Step 1 compute the function g and its limits $\lambda_{\min}(w)$ and $\lambda_{\max}(w)$. Step 2: Chose a nonlinear sector $z \in [z_1, z_2]$ and solve the LMI (31). Step 3 : design a linear observer (28) by pole placement. The whole control scheme to be implemented comprises the observer (28) , the control law (27), the change of variable (23), and finally the Hamiltonian minimization (15).

4. Simulation results

In this section, a simulation of the hybrid powertrain, shown in Fig. 1, is carried out using the quasi-LPV ECMS to obtain the control signal. Considering the bounds $z \in [-4.696\times10^{-7},\ -3.2021\times10^{-8}]$, the two controller gains are computed choosing a decay rate $\alpha = 1\times10^{-7}$ and the initial condition $X_0 = [0 \quad 0.425]^T$; whereas the observer gain is obtained by poles placement with poles -10 and -11. When solving the LMI conditions of proposition 1, the value of μ allows reaching different closed loop dynamics. Larger (resp. lower) μ values lead to larger (resp. lower) control gains $F_{1,2}$ and larger (resp. smaller) amplitude of the control signal $\dot{\lambda}$ in response to the exogenous signal w. The reference SOC signal $x_{ref}(t)$ varies from 100% down to a specified value with a rate limitation of $-0.75\%/h$.

From the PMP optimality conditions (16), $\dot{\lambda}$ should be kept as close to 0 as possible. In practice, a compromise has to be found between the SOC error and the hydrogen consumption. Several simulations have been conducted over the mission profile depicted in Fig. 2 for 15 linearly spaced values of μ and the final value of the reference signal is adjusted such that the actual final SOC is $x(T) = 20 \pm 0.1\%$. The quality of the SOC regulation is assessed through the RMS value of the SOC deviation $J_{\delta x}$:

$$J_{\delta x} = \sqrt{\frac{1}{T}\int_0^T \left(x(t) - x_{ref}(t)\right)^2 dt} \tag{35}$$

Obtained results are depicted in the Fig. 5 . As we focus on the H2 consumption minimization, the chosen value $\mu = 100$ is depicted with a vertical dashed line in the Fig. 5 .

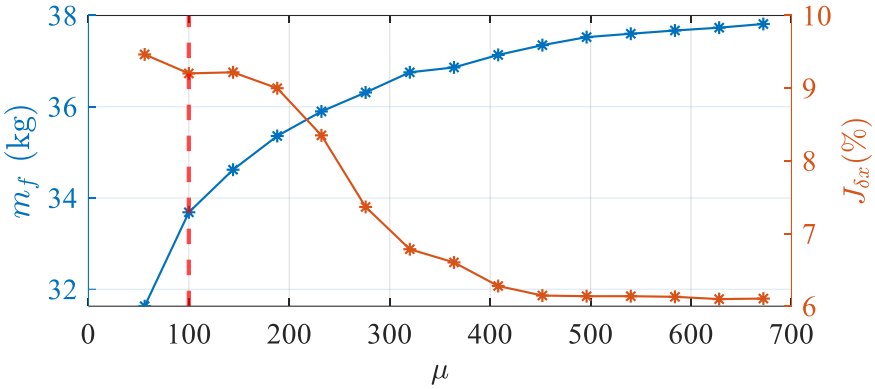

Fig. 5: Hydrogen consumption and $RMS(\dot{\lambda})$ as a function of μ .

For the particular case $\mu = 100$, by solving the LMI conditions of proposition 1, the following gains are obtained:

$$F_1 = \begin{bmatrix} 121.8 & 3.81\times10^{-4} \end{bmatrix}, \quad F_2 = \begin{bmatrix} 203.12 & 1.21\times10^{-3} \end{bmatrix},$$

$$L = \begin{bmatrix} 110 & 21 \end{bmatrix}, \quad P_1 = \begin{bmatrix} 5.09 & 1.45\times10^{-5} \\ 1.45\times10^{-5} & 3.389\times10^{-10} \end{bmatrix}.$$

In order to assess the effectiveness of our approach it is compared against the adaptive-ECMS strategy from (Onori et al., 2011), where the costate is computed as:

$$\lambda(k+1) = 0.5\left(\lambda(k) + \lambda(k-1)\right) + c_p\left(x - x_{ref}\right) \tag{36}$$

We chose $c_p = 100$ and a costate update period of 50 s. Fig. 6 depicts the comparison of the control input $u(t)$ and the battery power profile $y(t)$; it is shown how in the adaptive-ECMS strategy the control signal presents a bang-bang behaviour, whereas in the quasi-LPV ECMS the control signal is smoother; the corresponding evolution of the SOC is presented in Fig. 7. The obtained hydrogen consumption is $33.6\ kg$ for our approach and $41.68\ kg$ for the adaptive one.

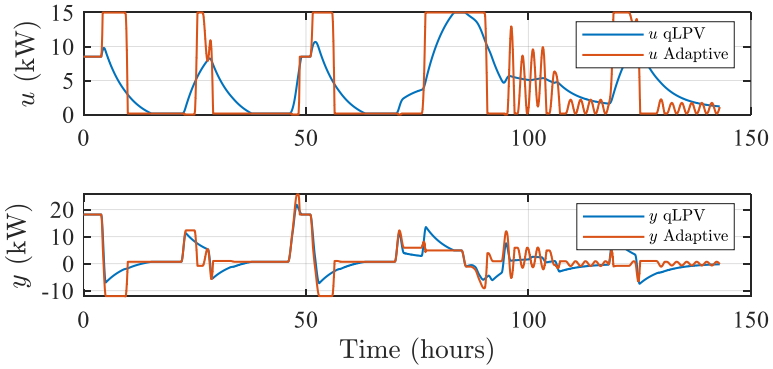

Fig. 6: Real time control law (simulation result).

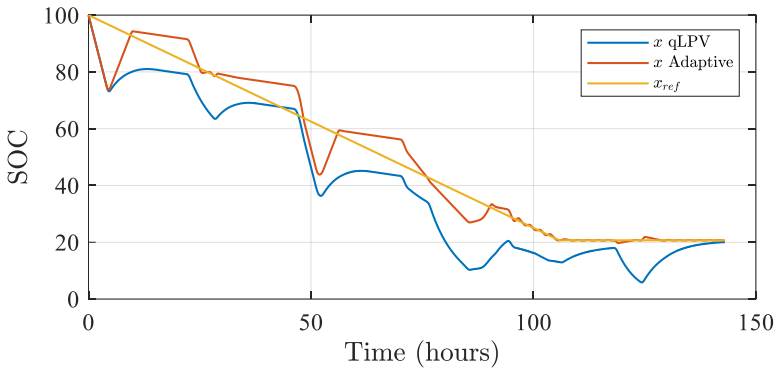

Fig. 7: SOC profiles comparison (simulation result).

5. Conclusions

A controller that benefits from the ECMS and quasi-LPV framework has been proposed. The controller synthesis is reduced to a set of LMI conditions to be solved. The closed loop ISS has been demonstrated. Preliminary results have been presented to illustrate the effectiveness of our approach. Two design parameters μ (related to a constraint on the costate derivative) and α (decay rate) allows tuning the closed loop dynamics. μ control the tradeoff between fuel consumption and state of charge regulation. Future work will be devoted to more in dept analysis of the control performances both in terms of fuel consumption and SOC reference tracking.

Acknowledgements

This work was supported in by the European Interreg Program through the Implentation of Hybrid Ship project ISHY) of the EU Interreg 2 seas program.

References

Abdelkrim, R., Wardi, M.L., Gassara, H., El Hajjaji, A., Chaabane, M., Abdelkrim, M.N., 2019. Relaxed Stabilization conditions for Takagi-Sugeno systems, in: 2019 16th International Multi-Conference on Systems, Signals Devices (SSD). Presented at the 2019 16th International Multi-Conference on Systems, Signals Devices (SSD), pp. 113–118.

Armenta, C., Delprat, S., Negenborn, R.R., Haseltalab, A., Lauber, J., Dambrine, M., 2022. Computational Reduction of Optimal Hybrid Vehicle Energy Management. IEEE Control Syst. Lett. 6, 25–30.

Bai, Y., Li, J., He, H., Santos, R.C.D., Yang, Q., 2020. Optimal Design of a Hybrid Energy Storage System in a Plug-In Hybrid Electric Vehicle for Battery Lifetime Improvement. IEEE Access 8, 142148–142158.

Boyd, S., El Ghaoui, L., Feron, E., Balakrishnan, V., 1994. Linear Matix Inequalities in system and control theory. SIAM.

East, S., Cannon, M., 2019. Fast Optimal Energy Management With Engine On/Off Decisions for Plug-in Hybrid Electric Vehicles. IEEE Control Syst. Lett. 3, 1074–1079. https://doi.org/10.1109/LCSYS.2019.2920164

Gao, H., Wang, Z., Yin, S., Lu, J., Guo, Z., Ma, W., 2021. Adaptive real-time optimal energy management strategy based on equivalent factors optimization for hybrid fuel cell system. Int. J. Hydrog. Energy 46, 4329–4338. https://doi.org/10.1016/j.ijhydene.2020.10.205

Guzzella, L., Sciarretta, A., 2005. Vehicle Propulsion Systems: Introduction to Modeling and Optimization. Springer-Verlag Berlin Heidelberg, New York (New York, USA).

Haseltalab, A., Negenborn, R.R., Lodewijks, G., 2016. Multi-Level Predictive Control for Energy Management of Hybrid Ships in the Presence of Uncertainty and Environmental Disturbances. IFAC-Pap., 14th IFAC Symposium on Control in Transportation SystemsCTS 2016 49, 90–95.

Hermant, A., 2008. On the shooting algorithm for optimal control problems with state constraints (Ph.D. Thesis). Ecole Polytechnique, Inria Saclay.

Kitzhofer, G., Koch, O., Pulverer, G., Simon, C., Weinmüller, E.B., 2010. The New MATLAB Code bvpsuite for the Solution of Singular Implicit BVPs.

Miyazaki, M.R., Sørensen, A.J., Lefebvre, N., Yum, K.K., Pedersen, E., 2016. Hybrid Modeling of Strategic Loading of a Marine Hybrid Power Plant With Experimental Validation. IEEE Access 4, 8793–8804.

Oncken, J., Chen, B., 2020. Real-Time Model Predictive Powertrain Control for a Connected Plug-In Hybrid Electric Vehicle. IEEE Trans. Veh. Technol. 69, 8420–8432. https://doi.org/10.1109/TVT.2020.3000471

Onori, S., Serrao, L., Rizzoni, G., 2011. Adaptive Equivalent Consumption Minimization Strategy for Hybrid Electric Vehicles. American Society of Mechanical Engineers Digital Collection, pp. 499–505.

Sampathnarayanan, B., Onori, S., Yurkovich, S., 2014. An optimal regulation strategy with disturbance rejection for energy management of hybrid electric vehicles. Automatica 50, 128–140. https://doi.org/10.1016/j.automatica.2013.11.006

Sanchez, M., Delprat, S., 2018. Hybrid Vehicle Energy Management: Avoiding the Explicit Hamiltonian Minimization, in: 2018 IEEE Vehicle Power and Propulsion Conference (VPPC). Presented at the 2018 IEEE Vehicle Power and Propulsion Conference (VPPC), pp. 1–5. https://doi.org/10.1109/VPPC.2018.8604992

Sciberras, E.A., Zahawi, B., Atkinson, D.J., Breijs, A., van Vugt, J.H., 2016. Managing Shipboard Energy: A Stochastic Approach Special Issue on Marine Systems Electrification. IEEE Trans. Transp. Electrification 2, 538–546. https://doi.org/10.1109/TTE.2016.2587682

Sontag, E.D., Wang, Y., 1996. New characterizations of input-to-state stability. IEEE Trans. Autom. Control 41, 1283–1294. https://doi.org/10.1109/9.536498

Tanaka, K., Wang, H.O., 2001. Fuzzy Control Systems Design and Analysis: A Linear Matrix Inequality Approach. John Wiley end Sons, Inc.

Tazelaar, E., Shen, Y., Veenhuizen, P.A., Hofman, T., van den Bosch, P.P.J., 2012. Sizing Stack and Battery of a Fuel Cell Hybrid Distribution Truck. Oil Gas Sci Technol – Rev IFP Energ. Nouv. 67, 563–573.

van Keulen, T., Gillot, J., de Jager, B., Steinbuch, M., 2014. Solution for state constrained optimal control problems applied to power split control for hybrid vehicles. Automatica 50, 187–192.

Wang, H.O., Tanaka, K., 2004. Fuzzy Control Systems Design and Analysis: A Linear Matrix Inequality Approach. John Wiley & Sons.

Wang, Jinbo, Wang, Jian, Yang, J., 2019. Simulation of Energy Control Strategy for Hybrid Electric Vehicle Based on Modified Dynamic Programming, in: 2019 3rd Conference on Vehicle Control and Intelligence (CVCI). pp. 1–4.

Xie, P., Tan, S., Guerrero, J.M., Vasquez, J.C., 2021. MPC-informed ECMS based real-time power management strategy for hybrid electric ship. Energy Rep., ICPE 2020-The International Conference on Power Engineering 7, 126–133.

Yoneyama, J., Nishikawa, M., Katayama, H., Ichikawa, A., 2000. Output stabilization of Takagi–Sugeno fuzzy systems. Fuzzy Sets Syst. 111, 253–266.